



Experimental and predicted excess molar enthalpies of some working pairs for absorption cycles

Raouf Zehioua^{a,b}, Christophe Coquelet^b, Chien-Bin Soo^b, Dominique Richon^{b,*},
Abdeslam-Hassen Meniai^a

^a Laboratoire de l'ingénierie des procédés de l'environnement (LIPE), Département de Chimie Industrielle, Université Mentouri Constantine, Route Ain El Bey, Constantine 25017, Algérie

^b MINES ParisTech, CEP/TEP - Centre énergétique et procédés, 35 Rue Saint Honoré, 77305 Fontainebleau, France

ARTICLE INFO

Article history:

Received 11 February 2009

Received in revised form 22 April 2009

Accepted 5 June 2009

Available online 16 June 2009

Keywords:

Excess enthalpies

C80 calorimeter

Redlich–Kister

Water

Ethanol

Glycol

Glycerol

UNIFAC

UNIQUAC

Absorption cycles

ABSTRACT

In this work, the measured excess molar enthalpies of absorption heat pump working pairs (refrigerant + absorbent), viz. water + mono-, di- and tri-ethylene glycol, water + glycerol, and ethanol + di- and tri-ethylene glycol mixtures are presented at 298.15 K and ambient pressure using a Setaram Calvet C80 calorimeter. The experimental results are represented and correlated by a Redlich–Kister type equation. Modeling of the excess enthalpies has been performed using the UNIFAC molecular group-contribution method, and UNIQUAC Gibbs energy model. In addition, the data and results are used to predict the Gibbs energy of all binary systems. This allows a preliminary evaluation of the suitability of the binary systems as heat pump working pairs.

© 2009 Elsevier B.V. All rights reserved.

1. Introduction

The knowledge of excess thermodynamic properties is very important in several industrial-related processes. These properties quantify the deviation from ideality of the thermodynamic functions of mixtures, which result essentially from molecular interactions. In industrial mixing processes, an understanding of the nature and magnitude of excess properties is mandatory.

A more specific industrial application of excess properties is the conception of an absorption heat pump. The usual methods to evaluate the performance of such pumps are based on the interaction and behavior of the two components making working pairs, i.e. a refrigerant, such as water or ethanol, with an absorbent—glycols or glycerol. According to the selection criteria for efficient working pairs, as listed by Narodoslowsky et al. [1] and Zheng et al. [2], dominant factors are the magnitude and location of the extremum of the excess Gibbs free energy function (g^E). Morrissey and O'Donnell [3] state that system pairs exhibiting highly negative deviations from Raoult's law give the best result. As a more refined guideline, a

strong non-ideality with a g^E extremum between: -1000 J/mol and -2000 J/mol located at high concentrations of the refrigerant, is usually recommended for good absorption heat pump performance [3]. Thus, the search for ideal working pairs requires the knowledge of excess Gibbs free energies of binary mixtures of refrigerants and absorbents, which is thermodynamically related to the excess enthalpy (h^E). Hence g^E can be easily obtained through experimental measurements of h^E thanks to a convenient solution model. Consequently, the aim of this work is to provide such datasets, which will be essential for the exergy analysis and the simulation of absorption heat pumps.

The polar–polar combination of water + glycol systems is known to exhibit negative excess enthalpies, essentially due to the presence of the hydroxyl group in both components. Molar excess enthalpies for the water + ethylene glycol (EG) system were measured by Rehm and Bittrich [4] at 298.15 K by thermometric titration, and later by Matsumoto et al. [5] at 298.15 K using an isothermal dilution calorimeter. Huot et al. [6] obtained water + EG h^E values from measurements of enthalpies of solution and of dilution at 298 K, although the values were more negative than both afore-mentioned references. More recently, Kracht et al. [7] used an LKB flow microcalorimeter for the same system and conditions. Their results compared favorably with that of Mat-

* Corresponding author. Tel.: +331 64 69 49 65; fax: +31 64 69 49 68.
E-mail address: dominique.richon@mines-paristech.fr (D. Richon).

Nomenclature

List of symbols

a	coefficients of the Redlich–Kister equation
g^E	excess molar Gibbs Free Energy (J/mol)
h^E	excess molar enthalpy (J/mol)
NG	number of subgroups
n	number of experimental points
P	pressure (Pa)
p	number of Redlich–Kister coefficients employed
Q_k	relative van der Waals surface area of subgroup in UNIFAC
q	molar surface parameter
R	universal gas constant ($R=8.314\text{ J (mol/K)}$)
R_k	relative van der Waals volume of subgroup in UNIFAC
r	molar volume parameter
s	excess molar entropy (J/mol)
T	temperature (K)
u	intermolecular energy (J/mol)
x	liquid mole fraction
\bar{x}	vector of liquid mole fractions
z	coordination number ($z=10$)

Greek letters

ϕ	segment fraction
γ	activity coefficient
v_k^i	number of groups of type k in molecule i
θ	area fraction
σ	standard deviation (J/mol, in this work)
Γ	residual activity coefficient

Superscripts

C	combinatorial contribution in UNIQUAC and UNIFAC theory
E	excess property
R	residual contribution in UNIQUAC and UNIFAC theory

Subscripts

cal	calculated property
exp	experimental property
i, j, k	dummy index for component i, j and k
m	melting

sumoto et al. in the water-rich region, although differences up to 5% were observed in the glycol region. Kracht et al. used, in addition to the conventional Redlich–Kister approach, the group-contribution models EBGCM and modified UNIFAC to describe qualitatively h^E curves. The deviation between the literatures water + EG results and our results have been calculated and listed in Table 8. Haman et al. [8] presented h^E values for water + di-ethylene glycol (DEG) and tri-ethylene glycol (TEG) at 298.15 K with an LKB flow microcalorimeter. For the Redlich–Kister equation, ethylene glycol does not require more than four coefficients, where five are generally used for the heavier glycols. To the best of our knowledge, no literature was found on ethanol+DEG or TEG systems, except for ethanol + EG at 298.15 K from Kracht et al. [9] and Nagashima et al. [10]. Adriana et al. [11] has measured h^E of EG + ethanol, DEG + ethanol and TEG + ethanol at 308.15 K by means of a flow microcalorimeter. Marcus [12] has calculated h^E values for the system water + glycerol using published data at 323 K and 343 K, and extrapolating them to 298 K using heat capacity data [13]. Huemer et al. [14] has measured excess molar enthalpies for water + glycerol

Table 1

Suppliers, purities and CAS numbers of the chemicals used.

Chemical	Supplier	Purity %	CAS number
Ethanol	Fluka	>99.8 (v/v)	64-17-5
Ethylene glycol	Sigma–Aldrich	>99 (GC)	107-21-1
Di-ethylene glycol	Sigma–Aldrich	>99 (GC)	111-46-6
Tri-ethylene glycol	Sigma–Aldrich	>99 (GC)	112-27-6
Glycerol	Sigma–Aldrich	>99 (GC)	56-81-5

at 323.15 K and 353.15 K up 2.5 MPa using a Calvet microcalorimeter (C-80 Setaram).

In this paper we present h^E values measured at 298.15 K and ambient pressure for the six working pairs, (water + EG, DEG, and TEG); (water + glycerol); and (ethanol + DEG and TEG), correlated by the empirical Redlich–Kister equation. Furthermore, we use our experimental results to optimize the binary interaction parameters within the solution model UNIQUAC, and along with the UNIFAC model, test their applicability and predictive capability concerning other excess thermodynamic properties.

2. Experimental

2.1. Materials

The chemicals were used as supplied without further purification, with the exception of water which was purified in the laboratory using a Millipore Direct-Q osmosis system. The chemical specifications are summarized in Table 1.

2.2. Apparatus

The Calvet C80 calorimeter, manufactured by SETARAM Instrumentation France, is a differential calorimeter based on the principles of Tian and Calvet [15]. It makes use of two batch, or continuous-operating, cells to measure differentially the evolution of heat with respect to a reference state.

The C80 calorimeter generally operates at atmospheric pressure up to 573 K, but can be also used for high pressure measurements [16]. It has two 12.5 cm³ cell wells, drilled into a central calorimetric block, to house the measurement and reference cells. Each well is equipped with its own flux-meter to monitor the heat flow around the cell during the experiment. Within the calorimetric block, a Pt100 platinum probe is used for monitoring the sample temperature. The temperature is accurately measured through one Pt200 platinum probe. Calibrations of the thermal probes have been achieved within the herein studied temperature range using reference melting temperatures of four standard materials; gallium ($T_m=302.91\text{ K}$); phenyl salicylate ($T_m=314.94\text{ K}$); biphenyl ($T_m=342.08\text{ K}$) and indium ($T_m=429.75\text{ K}$) [17]. The procedure related to the temperature calibration is clearly available elsewhere [15]. Upon extrapolation to 298 K, a maximum deviation of not more than 0.5 K should be expected for temperature, and not more than 1% for enthalpy. A sensitivity calibration of the thermopiles has been directly performed by the manufacturer upon installation of the calorimeter [17]. The entire calorimetric block is surrounded by a peripheral heating element, which regulates the sample temperature at a maximum rate of 1 K/min. This heating element is housed by a heat insulator. Stoppers and screws further acts as thermostated buffers for heat loss minimization. The entire calorimeter is mounted off the ground to a reversal stand, capable of 180° rotations. This automatism allows enhancing the mixing of liquids. Energy resulting from the rotation and consequently movement of the studied liquids has been verified to be negligible (less than 0.1 J) compared to measured mixing effects.

The mixing cells used for this work belong to the hastelloy cell type with membranes, which is specially adapted for the mixing of viscous fluids. It consists of a cylindrical body where two compartments can be isolated from each other using a membrane (Aluminum foil, 13 mm diameter 0.02 mm thick), Volume of each compartment is approximately 2.5 cm³. A rod, connected to a command rod, movable along the central shaft of the cell and the cell well, is used to break the membrane in order to mix the two liquids. The energy associated with the breaking of the membrane has been verified to be negligible (≈ 0.1 J).

2.3. Experimental procedure

The classical procedure that has been followed all along the measurements are described below. The temperature of the C80 calorimeter is stabilized at the required set point. A Mettler AT 200 analytical balance (max. 205 g), with a 0.1 mg maximum uncertainty, is used to weigh the masses introduced into the measurement cell. The reference cell is kept empty. The cells are then introduced into the calorimeter and isolated until the temperature and heat flow has stabilized as observed on the screen of the computer fitted with the SetSoft interface. Mixing is initiated via lowering the command rods of both cells and breaking the separation membrane, and followed by gentle rotation of the rod to aid mixing. Thereafter, both command rods are detached from the cell bodies and removed, and the reversal stand is activated to rotate the calorimeter through semi-circular arcs until the end of the experiment displayed by thermal signal stability. Integration of the heat flow peak yields the excess enthalpy, Measurements for each composition are repeated at least two times. Taking into account calibrations and reproducibility tests, we guarantee uncertainties less than 0.55 K for temperature, and 0.0002 for compositions. For enthalpy data we have made a comparison with results about hexane–cyclohexane system cited in [18] and found a maximum deviation of 3%. Furthermore we have made measurement of melting enthalpies of various compounds: gallium, phenyl salicylate, biphenyl and indium and found respectively maximum deviations of: 0.7%, 0.7%, 1.2% and 0.5%.

3. Excess thermodynamic properties representation

The experimental h^E data was fitted to a Redlich–Kister equation [19]:

$$h_{\text{cal}}^E = x_1(1 - x_1) \sum_{j=1}^n a_j(1 - 2x_1)^{j-1} \quad (1)$$

The quality of the fit is assessed via the standard deviation, given as:

$$\sigma = \sqrt{\frac{1}{(n-p)} \sum_{j=1}^n (h_{\text{exp}}^E - h_{\text{cal}}^E)^2} \quad (2)$$

where n is the number of experimental points, and p represents the number of Redlich–Kister coefficients used, with $n > p$ for all system measured. Furthermore, a useful way of analyzing excess enthalpies is to express them as h^E/x_1x_2 (related directly to the apparent molar enthalpies [20]), which will be studied in this work. We have used the Gibbs–Duhem equation:

$$g^E(T, P, \bar{x}) = RT \sum_i x_i \ln \gamma_i \quad (3)$$

to relate the excess enthalpy through the thermodynamic definition as follows:

$$h^E(T, P, \bar{x}) = \left\{ \frac{\partial [g^E/T]}{\partial [1/T]} \right\}_{P,x} = g^E - T \left\{ \frac{\partial g^E}{\partial T} \right\}_{P,x} \quad (4a)$$

Substituting Eq. (3), one gets:

$$h^E(T, P, \bar{x}) = -RT^2 \sum_i x_i \frac{\partial \ln \gamma_i}{\partial T} \quad (4b)$$

3.1. UNIQUAC method

The UNIQUAC (Universal Quasi Chemical) model was developed by Abrams and Prausnitz [21], and is based on the concept of two-liquid theory and the local composition model. The liquid phase activity coefficients are the sum of two terms; combinatorial and residual, where the former results from the differences between the size and structure of the molecules in the solution, and the latter from the interactions between the molecules:

$$\ln \gamma_i = \ln \gamma_i^C + \ln \gamma_i^R \quad (5)$$

$$= \left(\ln \frac{\phi_i}{x_i} + \frac{z}{2} q_i \ln \frac{\theta_i}{\phi_i} + l_i - \frac{\phi_i}{x_i} \sum_{j=1}^n x_j l_j \right) + q_i \left(1 - \ln \left(\sum_{j=1}^n \theta_j \tau_{ji} \right) - \sum_{j=1}^n \frac{\theta_j \tau_{ij}}{\sum_{k=1}^n \theta_k \tau_{kj}} \right) \quad (6)$$

Table 2

Molecular formulae of the species in this work, shown as structures of subgroups for group-contribution models.

Components	Molecular formula
Water H ₂ O	H ₂ O
Ethanol C ₂ H ₅ O	CH ₃ –CH ₂ –OH
Glycerol (propane-1,2,3-triol) C ₃ H ₈ O ₃	$\begin{array}{c} \text{CH}_2 - \text{CH} - \text{CH}_2 \\ \quad \quad \\ \text{OH} \quad \text{OH} \quad \text{OH} \end{array}$
Glycol (1,2-ethanediol) C ₂ H ₆ O ₂	$\begin{array}{c} \text{CH}_2 - \text{CH}_2 \\ \quad \\ \text{OH} \quad \text{OH} \end{array}$
Di-ethylene glycol C ₄ H ₁₀ O ₃	$\begin{array}{c} \text{CH}_2 - \text{CH}_2\text{O} - \text{CH}_2 - \text{CH}_2 \\ \quad \quad \quad \\ \text{OH} \quad \quad \quad \text{OH} \end{array}$
Tri-ethylene glycol C ₆ H ₁₄ O ₄	$\begin{array}{c} \text{CH}_2 - \text{CH}_2\text{O} - \text{CH}_2 - \text{CH}_2\text{O} - \text{CH}_2 - \text{CH}_2 \\ \quad \quad \quad \quad \quad \quad \\ \text{OH} \quad \quad \quad \text{OH} \quad \quad \quad \text{OH} \end{array}$

Table 3

Subgroup parameters for the UNIQUAC and UNIFAC models [22]. Indicated also are the two possibilities of subgroup combinations for each of the three glycols in this paper.

Subgroup	R_k	Q_k	EG		DEG		TEG	
			Option 1	Option 2	Option 1	Option 2	Option 1	Option 2
CH ₂	0.674	0.540	2		3	2	4	2
OH	1.000	1.200	2		2	1	2	
H ₂ O	0.920	1.400						
CH ₂ O	0.918	0.780			1		2	
DOH	2.409	2.248		1				
OCCOH	2.123	1.904				1		2

The two adjustable interaction parameters, τ_{ij} and τ_{ji} , can be further expressed as a function of intermolecular energy U_{ij} between like and unlike molecules of i and j :

$$\tau_{ij} = \exp\left(-\frac{u_{ij} - u_{jj}}{RT}\right) \text{ and } \tau_{ji} = \exp\left(-\frac{u_{ji} - u_{ii}}{RT}\right) \quad (7)$$

where $u_{ij} = u_{ji}$. Since for the UNIQUAC model (as well as the UNIFAC) the temperature dependency lies solely in the residual term, the expression of excess enthalpy is then obtained by the following equation:

$$h^E(T, P, \bar{x}) = -\left(RT^2 \sum_i x_i \frac{\partial \ln \gamma_i^R}{\partial T}\right) \quad (8)$$

3.2. UNIFAC method

Developed by Fredenslund et al. [22], the UNIFAC (Universal Functional Activity Coefficient) model is based on the concept that each fluid mixture is regarded as a solution of structural units, or *subgroups*, which collectively construct into the molecules that make up the fluid. Table 2 gives the molecular structures of the chemicals in this work, as formed by various subgroups. While the liquid phase activity coefficients are similar to that of UNIQUAC (combinatorial + residual terms as in Eq. (5)), the effects are defined in terms of subgroups, rather than entire molecules:

$$\ln \gamma_i = \ln \gamma_i^C + \ln \gamma_i^R = \left(\ln \frac{\phi_i}{x_i} + \frac{z}{2} q_i \ln \frac{\theta_i}{\phi_i} + l_i - \frac{\phi_i}{x_i} \sum_{j=1}^{NG} x_j l_j \right) + \sum_{k=1}^{NG} v_k^i (\ln \Gamma_k - \ln \Gamma_k^i) \quad (9)$$

For the three glycols, one observes that there are two combinations in which each glycol may be constructed by the subgroups. Table 3 shows the two possibilities of decomposition for each glycol using UNIFAC subgroups, along with the subgroup parameters used in this work [23]. Additional parameters, such as group–group interaction parameters, that are not given in the table can be found in Ref. [23].

3.3. Parameter determination

The least squares method was used to determine the fitting coefficients of the Redlich–Kister equation, with an optimal number of parameters determined by increasing the number of coefficients until σ is no longer significantly improved. The binary UNIQUAC parameters were fitted for each of the six measured systems, using the SimulisTM software package (from Prosim, Toulouse, France) and Microsoft ExcelTM, for the minimization of the following objec-

Table 4

Excess molar enthalpies for water + glycols and glycerol binary systems at 298.15 K.

x_1	h_{exp}^E (J/mol)	x_1	h_{exp}^E (J/mol)	x_1	h_{exp}^E (J/mol)
Water (1)–ethylene glycol (2)					
0.1014	–174	0.3995	–590	0.7949	–681
0.1994	–337	0.4807	–640	0.8656	–570
0.2091	–347	0.5455	–666	0.9150	–423
0.3051	–480	0.6144	–698		
0.3674	–559	0.6690	–715		
Water (1)–di-ethylene glycol (2)					
0.1026	–275	0.4937	–1039	0.8999	–857
0.2012	–511	0.5018	–1066	0.9002	–867
0.2094	–521	0.6003	–1192	0.9498	–538
0.3067	–741	0.6996	–1245		
0.4068	–931	0.7998	–1172		
Water (1)–tri-ethylene glycol (2)					
0.1291	–440	0.4016	–1340	0.6999	–1876
0.2167	–787	0.5006	–1606	0.7985	–1767
0.3145	–1079	0.6006	–1803	0.9013	–1307
Water (1)–glycerol (2)					
0.1028	–152	0.3964	–471	0.6991	–611
0.2192	–292	0.5022	–547	0.8005	–560
0.3038	–387	0.5956	–598	0.8995	–364

tive function:

$$F = \frac{100}{n} \sum_{i=1}^n \left[\frac{h_{i,\text{exp}}^E - h_{i,\text{cal}}^E}{h_{i,\text{exp}}^E} \right]^2 \quad (10)$$

4. Results and discussion

The measured excess molar enthalpy data for the {Water (1)+EG (2)}, {Water (1)+DEG (2)}, {Water (1)+TEG (2)}, {Water (1)+Glycerol (2)}, {Ethanol (1)+DEG (2)}, and {Ethanol (1)+TEG (2)} systems at $T = 298.15$ K are reported in Tables 4 and 5. The optimized parameters for the Redlich–Kister and UNIQUAC models are listed in Tables 6 and 7.

4.1. Water + Glycols/Glycerol systems

Fig. 1 shows the experimental excess enthalpies of the water + glycols and + glycerol systems, plotted with their respec-

Table 5

Excess molar enthalpies for ethanol + DEG and TEG binary systems at 298.15K.

x_1	h_{exp}^E (J/mol)	x_1	h_{exp}^E (J/mol)	x_1	h_{exp}^E (J/mol)
Ethanol (1)–di-ethylene glycol (2)					
0.1048	76	0.4009	249	0.7041	252
0.1991	129	0.4963	262	0.7958	204
0.2967	193	0.5879	280	0.9006	121
Ethanol (1)–tri-ethylene glycol (2)					
0.1040	117	0.5002	494	0.8992	260
0.2042	245	0.5990	508		
0.3010	350	0.6993	470		
0.3990	435	0.7995	403		

Table 6

Values of coefficients for Redlich–Kister and given standard deviations for the six studied binary systems at 298.15 K. (A) Water + EG; (B) Water + DEG; (C) Water + TEG; (D) Water + Glycerol; (E) Ethanol + DEG; (F) Ethanol + TEG.

System	a_1	a_2	a_3	a_4	a_5	σ (J/mol)
A	-2605	1177	-1545	1552	-	7.3
B	-4292	2693	-2153	2280	-1598	7.9
C	-6415	4417	-2888	3385	-2350	23.2
D	-2193	1336	-1062	319	-	5.6
E	1	1076	-346	-31	-	6.3
F	1956	-652	119	-556	-	4.9

Table 7

Interaction parameters for the UNIQUAC model between different components, fitted to experimental h^E data.

i	j	$u_{ij}-u_{ji}$ (J/mol)	$u_{ji}-u_{ii}$ (J/mol)	σ (J/mol)
Water	EG	159.2	-412.9	26.2
Water	DEG	-18.9	-429.1	17.3
Water	TEG	-133.2	-468.5	29.0
Water	Glycerol	19.9	-265.4	11.5
Ethanol	EG	276.2	-27.5	4.0
Ethanol	DEG	75.8	28.2	9.1
Ethanol	TEG	105.6	69.2	16.6

tive optimized Redlich–Kister equations. Negative, exothermic h^E 's are exhibited for the entire range of compositions for all four systems. A global minimum close to $x_{\text{water}}=0.7$ is observed in each case. Although the data appears slightly skewed, the modified form of the Redlich–Kister equation [24] was tested for all systems, and give similar or slightly higher standard deviations.

The negative value of h^E is attributed to the formation of hydrogen bonds between the glycols or glycerol, and water (hydrophilic hydration, [25]). The addition of ether-groups ($-\text{CH}_2\text{O}$) in DEG and TEG makes the excess enthalpies more negative. This can be due to the additional oxygen, readily available for further hydrogen bonding. At the same time, a hydrophobic hydration between alkyl groups ($-\text{CH}_2$) and $-\text{OH}$ groups, may exist and result in a positive contribution to the excess enthalpies. However, the fact that strongly negative h^E still prevails is an indication of the dominance of the hydrophilic hydration in the systems. One may suggest that with three $-\text{OH}$ groups, the h^E values of the water + glycerol system would rank among those of DEG, rather than being similar to EG. This was explained by Jonsdottir and Klein [26], who observed a similarity between the interactions of the systems water + EG

and water + glycerol when the interaction energies and configurations are computed by molecular mechanics methods. In general, the large number of Redlich–Kister coefficients required (four or more) is an indication of the specific interactions that are present in these systems. In addition to the number of oxygen atoms and alkyl groups, the length and branching of the molecules of glycols or glycerol may also greatly influence the hydrophilic behavior. As shown in Table 2, the branching for the glycols is at the extremities of the main 'skeleton' of the molecule (at the terminal groups), whereas for the glycerol molecule branching is at terminal and intermediate groups. This may explain the fact that, although the oxygen atom concentration in molecules of glycols and glycerol is the same (50%), the excess molar enthalpies of the three glycols are always greater in absolute value than that of glycerol, since the former provide more 'room' and ease for water molecules to form hydration cages, contrary to glycerol molecules where water molecules may find difficulties in bonding due to repulsive forces possibly induced by the intermediate branching, at short distances to alkyl groups. Within the glycols class, clearly the greater the number of oxygen atoms present, the greater is the excess molar enthalpy in absolute value. For a constant water composition, it is interesting to relate these two parameters (number of oxygen atoms and h^E). The fact that the hydrophilic character dominates the hydrophobic one, can be explained by the ease found by the water molecules to orientate themselves around the glycol molecules so that the system energy would be at minimum (negatively) "hence" minimizing the eventual repulsive effects with the alkyl groups. This is supported by molecular energy calculations performed by Menai and Newsham [27].

The plots of h^E/x_1x_2 (Fig. 2) seem to indicate that hydrophobic interactions may occur in the very dilute water region. This phenomenon is similar to that pointed out by Perron et al. [28] for the *tert*-butanol–water mixture, however measurements in the very dilute region are necessary to confirm this assumption. Nonetheless, as a verification using isothermal vapor–liquid equilibrium data [29], g^E was calculated for water + EG at 298.15 K. The calculated g^E values are small and this instead proves the coexistence of compensating entropic and molecular interaction effects which are not characteristic of regular ($|h^E| \gg T|s^E|$, $g^E \approx h^E$) or athermal ($|h^E| \ll T|s^E|$, $g^E \approx -T \cdot s^E$) solutions.

Figs. 3–10 show the excess enthalpies and Gibbs free energy of the water + glycol and + glycerol system as predicted by UNIFAC and calculated by UNIQUAC with the optimized parameters. Comparisons with literature data is plotted alongside UNIFAC model

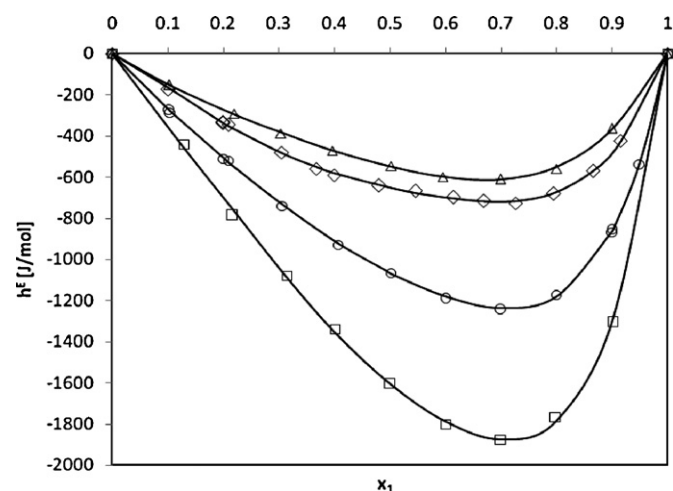


Fig. 1. Excess molar enthalpies at 298.15 K and atmospheric pressure for: (◇) water (1) + EG (2); (○) water (1) + DEG (2); (□) water (1) + TEG (2) and (△) water (1) + glycerol (2). Solid line: Redlich–Kister equation.

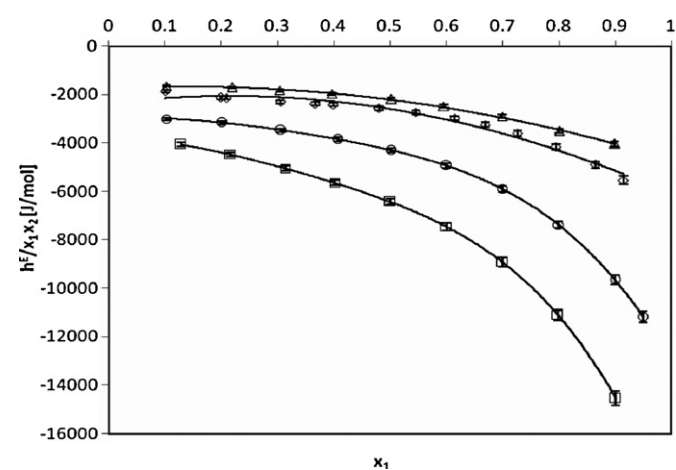


Fig. 2. Total apparent molar enthalpies at 298.15 K and atmospheric pressure for: (◇) water (1) + EG (2); (○) water (1) + DEG (2); (□) water (1) + TEG (2) and (△) water (1) + glycerol (2). Error bars shown at $\pm 3\%$. Solid lines are second order polynomial tendency curves.

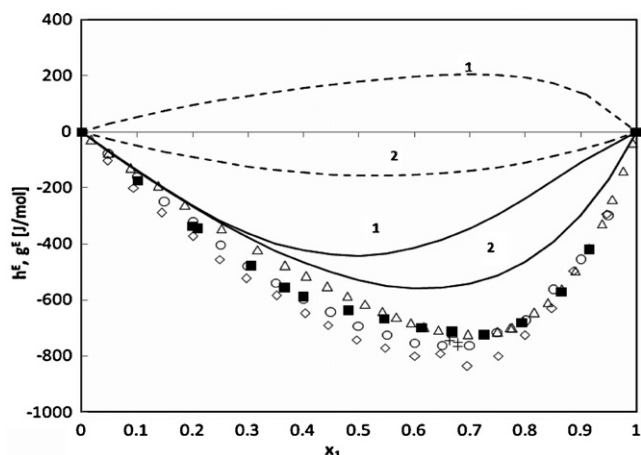


Fig. 3. Excess molar enthalpies at 298.15 K and atmospheric pressure for water (1)+EG (2): (■) this work; (+) Rehm and Bittrich [4]; (Δ) Matsumoto et al. [5]; (\diamond) Huot et al. [6]; (\circ) Kracht et al. [7]; dashed line: g^E UNIFAC; solid line: h^E UNIFAC. 1 denotes option 1 of UNIFAC subgroup definition, and 2 denoted group 2, as listed in Table 3.

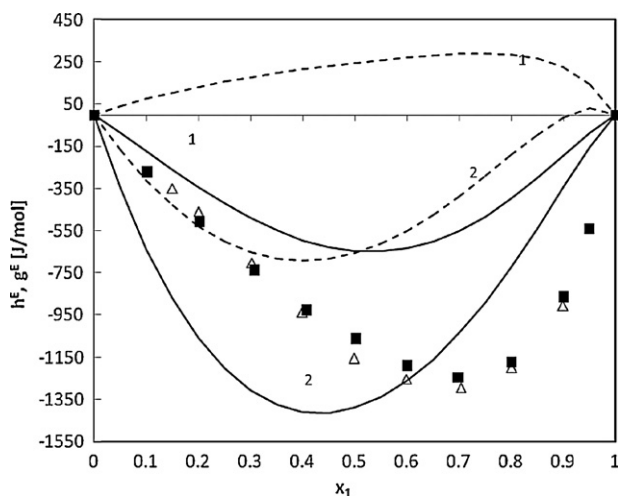


Fig. 4. Excess molar enthalpies at 298.15 K and atmospheric pressure for water (1)+DEG (2): (■) this work; (Δ) Haman et al. [8]; dashed line: g^E UNIFAC; solid line: h^E UNIFAC. 1 denotes option 1 of UNIFAC subgroup definition, and 2 denoted group 2, as listed in Table 3.

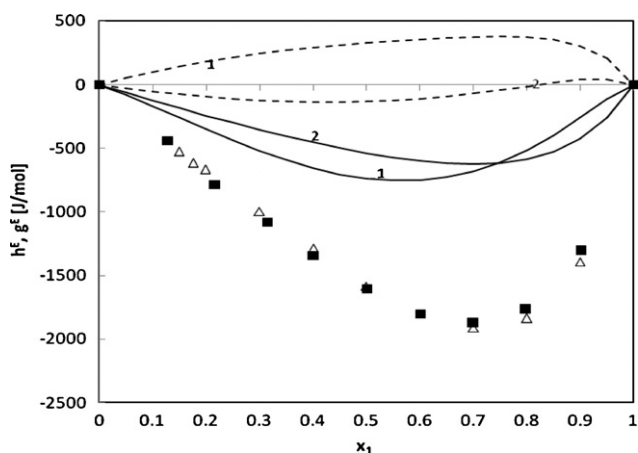


Fig. 5. Excess molar enthalpies at 298.15 K and atmospheric pressure for water (1)+TEG (2): (■) this work; (Δ) Haman et al. [8]; dashed line: g^E UNIFAC; solid line: h^E UNIFAC. 1 denotes option 1 of UNIFAC subgroup definition, and 2 denoted group 2, as listed in Table 3.

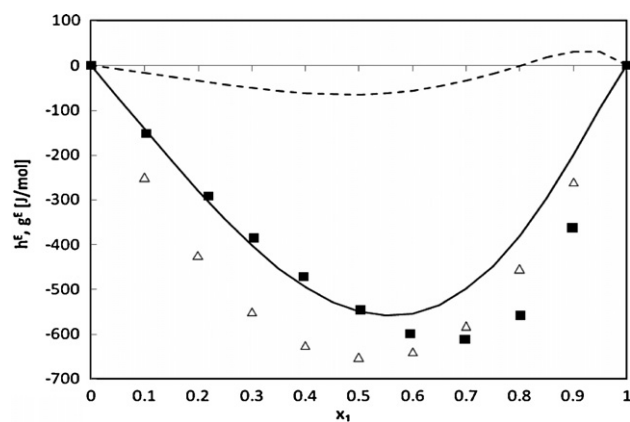


Fig. 6. Excess molar enthalpies at 298.15 K and atmospheric pressure for water (1)+glycerol (2): (■) this work; (Δ) extrapolated h^E values by Marcus [11]; dashed line: g^E UNIFAC; solid line: h^E UNIFAC. 1 denotes option 1 of UNIFAC subgroup definition, and 2 denoted group 2, as listed in Table 3.

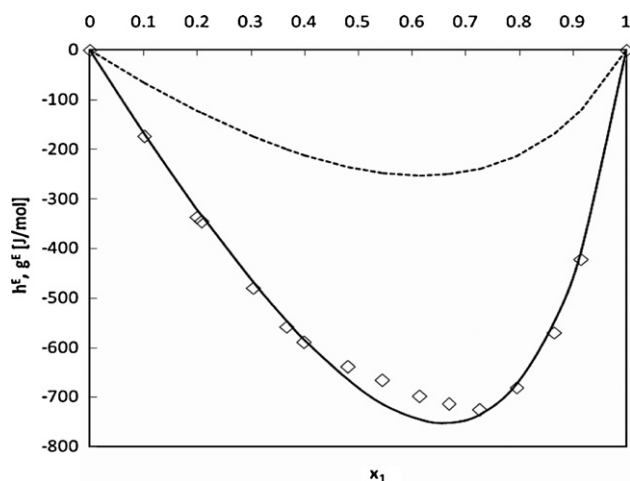


Fig. 7. Excess molar enthalpies at 298.15 K and atmospheric pressure for water (1)+EG (2): (\diamond) experimental results; solid line: h^E and dashed line: g^E correlated and predicted by UNIQUAC, using optimized parameters.

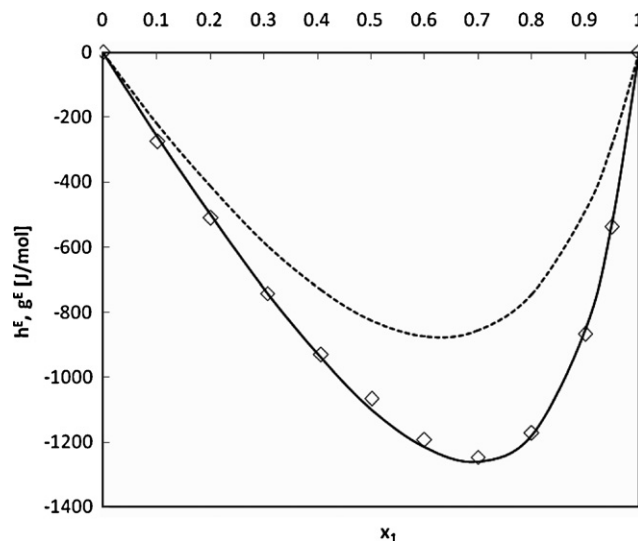


Fig. 8. Excess molar enthalpies at 298.15 K and atmospheric pressure for water (1)+DEG (2): (\diamond) experimental results; solid line: h^E and dashed line: g^E correlated and predicted by UNIQUAC, using optimized parameters.

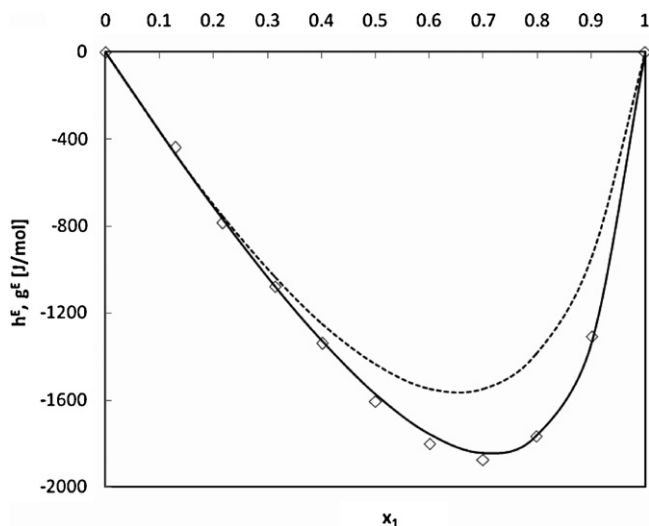


Fig. 9. Excess molar enthalpies at 298.15 K and atmospheric pressure for water (1) + TEG (2): (\diamond) experimental results; solid line: h^E and dashed line: g^E correlated and predicted by UNIQUAC, using optimized parameters.

calculations. The relative absolute deviations between the literature {Water (1)+EG (2)}, {Water (1)+DEG (2)}, {Water (1)+TEG (2)} results, our results and those obtained using the optimized Redlich–Kister parameters have been calculated and are listed in Table 8. Only a rough similarity appear between data presented via indirect methods [6] and extrapolations [12]. UNIFAC is clearly inapt in predicting h^E and g^E of all the four systems, whatever the chosen option. The two options of the subgroup configurations of glycols dictate the number and frequency of subgroup–subgroup possible interactions. For example, option 2 of all three glycols generally leads to more negative values for all water + glycol systems. This may be due to the fact that the alkyl group (subgroup $-\text{CH}_2$), which contributes positively to h^E , is combined with other subgroups to form larger subgroups, which in turn may contribute negatively. On the contrary, option 1 involves each present alkyl group explicitly (two for EG, three for DEG, four for TEG); thus their positive contribution is not “masked”, as it is in option 2. On the other hand, UNIQUAC is able to represent the excess enthalpy reasonably well.

It is difficult to evaluate the nature of the g^E values by means of UNIFAC due to its lack of predictive reliability for these sys-

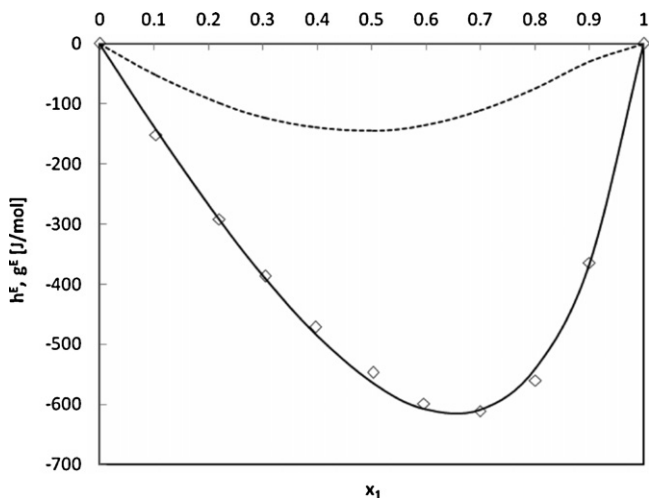


Fig. 10. Excess molar enthalpies at 298.15 K and atmospheric pressure for water (1) + glycerol (2): (\diamond) experimental results; solid line: h^E and dashed line: g^E correlated and predicted by UNIQUAC, using optimized parameters.

Table 8

The relative absolute deviation* of experimental results of this work and literature data, using optimized Redlich–Kister coefficients as given in Table 6.

Results	Relative deviation/%
Water (1)+EG (2)	
This work	1
Rehm and Bittrich [4]	4
Matsumoto et al. [5]	12
Huot et al. [6]	9
Kracht et al. [7]	4
Water (1)+DEG (2)	
This work	3
Haman et al. [8]	6
Water (1)+TEG (2)	
This work	1
Haman et al. [8]	3

$$\frac{100}{n} \times \sum \left(\frac{h^E, \text{exp} - h^E, \text{cal}}{h^E, \text{exp}} \right)$$

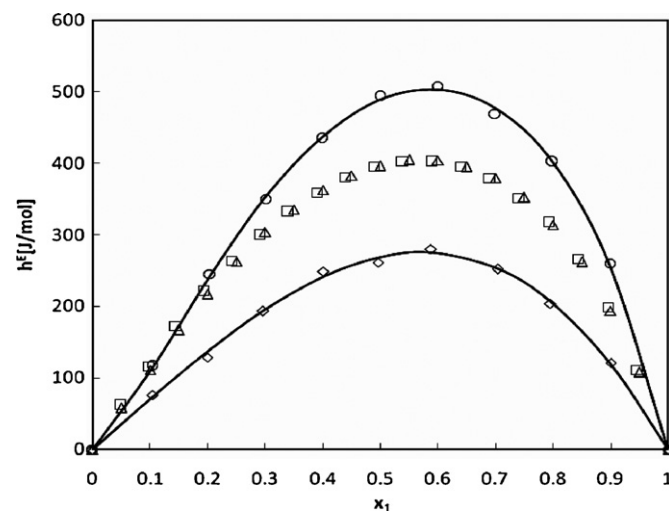


Fig. 11. Excess molar enthalpies at 298.15 K and atmospheric pressure: (\diamond) ethanol (1) + DEG (2) and (\circ) ethanol (1) + TEG (2); (Δ) ethanol (1) + EG (2) from Kracht et al. [9], (\square) ethanol (1) + EG (2) from Nagashima et al. [10]. Solid line: Redlich–Kister equation.

tems, but it can be seen through the UNIQUAC correlations that water + TEG, and to a less extent the remaining water binary systems, fit the requirements for possible heat pump working pairs, i.e., highly negative g^E values, as mentioned previously. This will be verified through calculations of machine performance criteria such as the coefficient of performance (COP) in a future work.

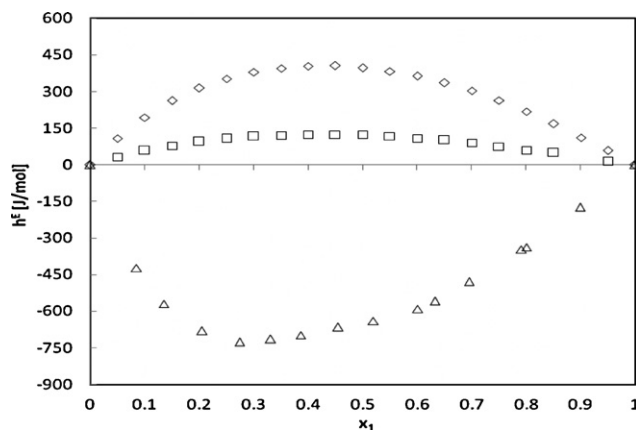


Fig. 12. Excess molar enthalpies at 298.15 K and atmospheric pressure for the systems (\square) water (1) + EG (2) from this study; and (Δ) methanol (1) + EG (2) and (\diamond) ethanol (1) + EG (2) from Kracht et al. [9].

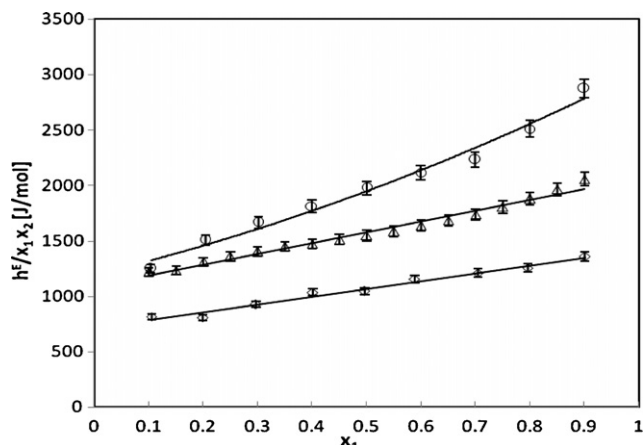


Fig. 13. Total apparent molar enthalpies at 298.15 K and atmospheric pressure for: (Δ) ethanol (1)+EG (2); (\diamond) ethanol (1)+DEG (2); (\circ) ethanol (1)+TEG (2). Error bars shown at $\pm 3\%$. Solid lines are second order polynomial tendency curves.

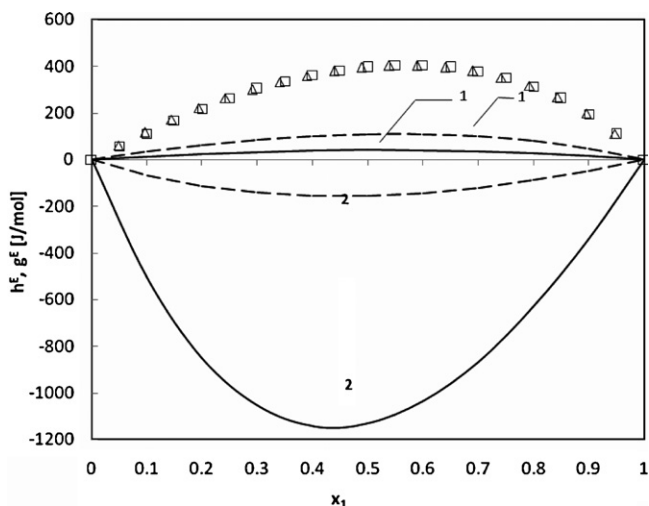


Fig. 14. Excess molar enthalpies at 298.15 K and atmospheric pressure for ethanol (1)+EG (2): (\square) Kracht et al. [9], (Δ) ethanol (1)+EG (2) from Nagashima et al. [10]; dashed line: g^E UNIFAC; solid line: h^E UNIFAC. 1 denotes option 1 of UNIFAC subgroup definition, and 2 denoted group 2, as listed in Table 3.

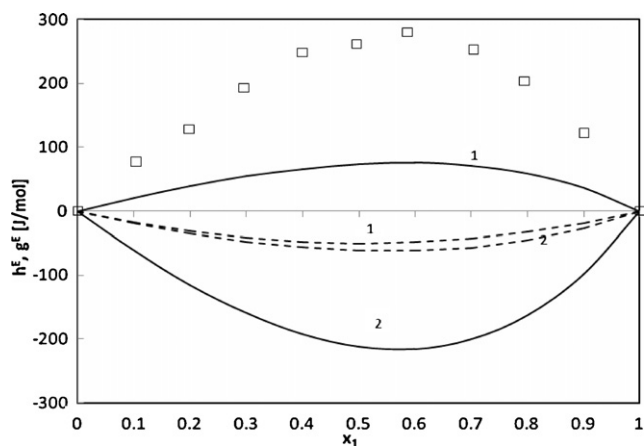


Fig. 15. Excess molar enthalpies at 298.15 K and atmospheric pressure for ethanol (1)+DEG (2): (\square) experimental results; dashed line: g^E UNIFAC; solid line: h^E UNIFAC. 1 denotes option 1 of UNIFAC subgroup definition, and 2 denoted group 2, as listed in Table 3.

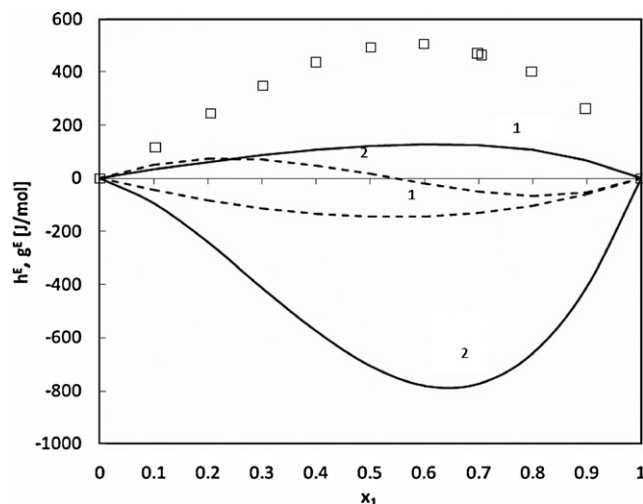


Fig. 16. Excess molar enthalpies at 298.15 K and atmospheric pressure for ethanol (1)+TEG (2): (\square) experimental results; dashed line: g^E UNIFAC; solid line: h^E UNIFAC. 1 denotes option 1 of UNIFAC subgroup definition, and 2 denoted group 2, as listed in Table 3.

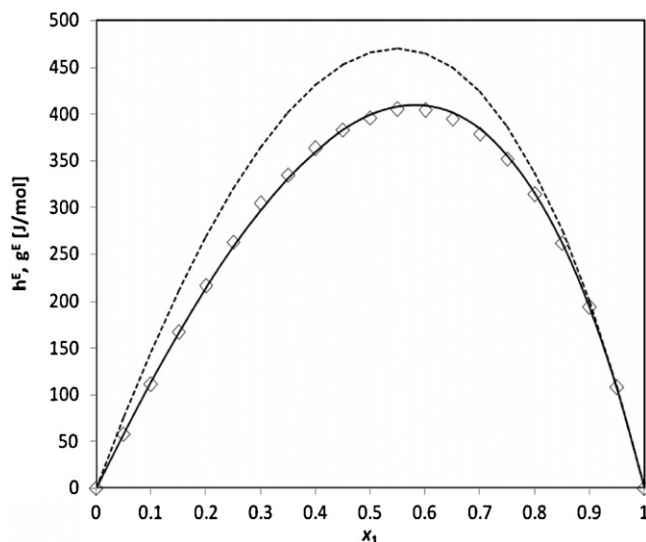


Fig. 17. Excess molar enthalpies at 298.15 K and atmospheric pressure for ethanol (1)+EG (2): (\diamond) experimental results of Kracht et al. [9]; solid line: h^E and dashed line: g^E correlated and predicted by UNIQUAC, using optimized parameters.

4.2. Ethanol + Glycols systems

The experimental excess enthalpies for the ethanol + glycol systems are positive for the entire composition range, as illustrated in Fig. 11. The maximum h^E occurs at close to $x_{\text{EtOH}} = 0.6$ for all three systems, including the data of Kracht et al. [9]. In these systems, the negative hydrophilic contributions from the $-\text{OH}$ group of an ethanol molecule is smaller compared to that of water, due to its dilution by alkyl groups of the same alcohol molecule. In addition, the linear chain structure of ethanol molecules compared to water makes it slightly more difficult for bond formations because of steric hindrance; thus less hydrogen bonds are formed. It may also be possible that the net negative contribution is smaller than the total heat absorbed for the breakup of the self-association between ethanol molecules, thus yielding an overall positive, endothermic excess enthalpy. The evolution of h^E in ethanol + glycol systems with each subsequent level of glycol is somewhat different to that of the water + glycol systems. With the addition of a $\text{CH}_2\text{O}-\text{CH}_2$ group from EG to DEG, the increase in the energy required for the destruc-

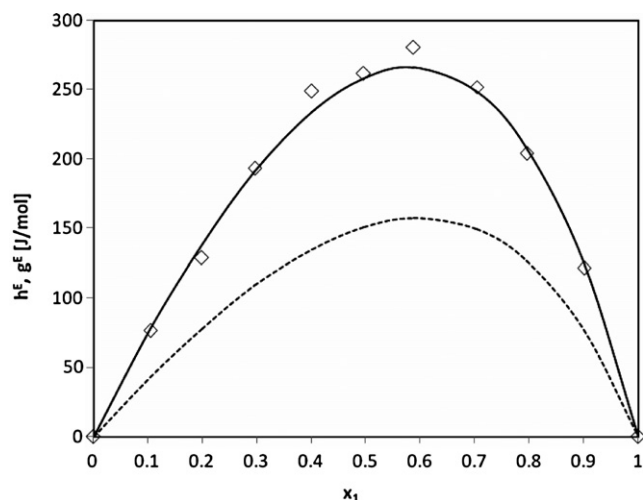


Fig. 18. Excess molar enthalpies at 298.15 K and atmospheric pressure for ethanol (1) + DEG (2): (\diamond) experimental results; solid line: h^E and dashed line: g^E correlated and predicted by UNIQUAC, using optimized parameters.

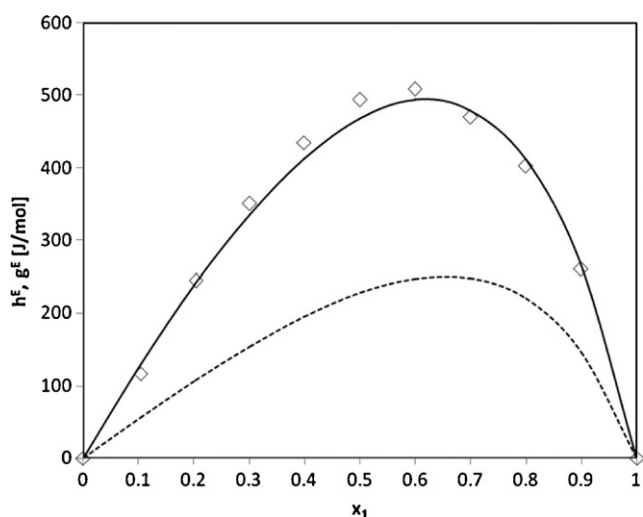


Fig. 19. Excess molar enthalpies at 298.15 K and atmospheric pressure for ethanol (1) + TEG (2): (\diamond) experimental h^E results; solid line: h^E and dashed line: g^E correlated and predicted by UNIQUAC, using optimized parameters.

tion of self-association complexes is smaller than the increase in energy released from ether-group hydrogen bonding; thus less positive h^E results. This is however inverted with TEG, where the energy absorbed for bond-breaking greatly exceeds the slightly weaker negative energy release from the ethanol –OH bonds, as compared to water –OH bonds.

In Fig. 12, the excess enthalpies of the systems EG + water, + methanol [9], and + ethanol are plotted together at 298 K to demonstrate the presence of alkyl groups on hydrophilic effects. The excess enthalpies increase, from initially negative with water, to positive as the numbers of carbons and methyl groups increase, weakening the negative hydrophilic effects.

For ethanol systems plotted as h^E/x_1x_2 vs x_1 (Fig. 13), we observe quasi linear behaviors. This is certainly due to smaller polarity of ethanol with respect to water. Consequently, fewer parameters are necessary for good correlation through Redlich–Kister equation.

Similarly to water + glycol systems, UNIFAC failed in predicting accurately h^E and g^E values, as shown in Figs. 14–16. Once

more option 2 lead to negative h^E , except that the differences are much bigger. Clearly UNIQUAC is our recommended model for the correlation of these systems (see Figs. 17–19). However, none of the ethanol + glycol systems give the negative Gibbs free energy required for effective heat pump working pairs.

5. Conclusions

Excess enthalpies of water + glycols (mono-, di- and tri-ethylene glycol), ethanol + glycols (di- and tri-ethylene glycol) and water + glycerol mixtures were measured at 298 K and atmospheric pressure using a Calvet C80 calorimeter. The experimental values have been fitted to the Redlich–Kister equation and the UNIQUAC model. A comparison between the predictive UNIFAC, and the two parameter UNIQUAC model, shows that the latter is more reliable in both correlating and predicting the considered excess properties.

Based on the Morrissey and O'Donnell approach, water + mono-, di-, tri-ethylene glycol and glycerol may be used as suitable working pairs for absorption heat pumps. However, tri-ethylene glycol appears to be slightly better than the others, having the most negative excess Gibbs energy as predicted by the UNIQUAC model. The positive excess Gibbs energies of ethanol + mono-, di-, and tri-ethylene glycol suggest to discard these systems as working pairs, although more detailed analyses and simulations are required for definite conclusions, possibly in a future study.

Acknowledgements

The authors would like to thank Dr. D. Dalmazzone and professor F. Belaribi for their invaluable advices on calorimetric measurements and the region “île de France” (SESAME) for its financial support.

References

- [1] M. Narodoslawsky, G. Otter, F. Moser, Heat recovery systems CHP 8 (5) (1988) 459–468.
- [2] D. Zheng, P. Ji, J. Qi, Int. J. Refrigeration 24 (2001) 834–840.
- [3] A.J. Morrissey, J.P. O'Donnell, Chem. Eng. Res. Des. 64 (1986) 404–406.
- [4] K. Rehm, H.-J. Bittrich, Z. Phys. Chem. 251 (1972) 109–121.
- [5] Y. Matsumoto, H. Touhara, K. Nakanishi, N. Watanabe, J. Chem. Therm. 9 (1977) 801–805.
- [6] J.-Y. Huot, E. Battistel, R. Lumry, G. Villeneuve, J.-F. Lavallee, A. Anusiem, C. Jolicœur, J. Solution Chem. 17 (1988) 601–631.
- [7] C. Kracht, P. Ulbig, S. Schulz, J. Chem. Therm. 31 (1999) 1113–1127.
- [8] S.E.M. Haman, G.C. Benson, M.K. Kumaran, J. Chem. Therm. 17 (1985) 973–976.
- [9] C. Kracht, P. Ulbig, S. Schulz, Thermochim. Acta 337 (1999) 209–217.
- [10] A. Nagashima, S. Yoshii, H. Matsuda, K. Ochi, J. Chem. Eng. Data 49 (2004) 286–290.
- [11] A. Bigi, F. Comelli, Thermochim. Acta 430 (2005) 191–195.
- [12] Y. Marcus, Phys. Chem. Chem. Phys. 2 (2000) 4891–4896.
- [13] H. Huemer, E. Platzer, K. Rehak, Thermochim. Acta 187 (1991) 95–112.
- [14] H. Huemer, E. Platzer, K. Rehak, Thermochim. Acta 231 (1994) 21–30.
- [15] E. Calvet, H. Part, H.A. Skinner, Recent Progress in Microcalorimetry, Pergamon Press, New York, 1963.
- [16] S. Schrödle, E. Königsberger, P.M. May, G. Heffer, Geochim. et Cosmochim. Acta 72 (2008) 3124–3138.
- [17] Setaram® Calvet C80 Calorimeter User Manual–Commissioning, 2005.
- [18] K.N. Marsh, R.H. Stokes, J. Chem. Therm. 1 (1969) 223–225.
- [19] O. Redlich, A.T. Kister, Ind. Eng. Chem. 40 (1948) 345–348.
- [20] J.E. Desnoyers, G. Perron, J. Solution Chem. 26 (1997) 749–755.
- [21] D.S. Abrams, J.M. Prausnitz, AIChE. J. 21 (1975) 116–128.
- [22] A. Fredenslund, R.L. Jones, J.M. Prausnitz, AIChE. J. 21 (1975) 1086–1099.
- [23] J.D. Raal, A.L. Mühlbauer, Phase Equilibria: Measurement and Computation, Taylor & Francis, Washington, 1999.
- [24] K.N. Marsh, J. Chem. Therm. 9 (1977) 719–724.
- [25] F. Franks, D.J.G. Ives, Quart. Rev. 20 (1966) 1–44.
- [26] S.O. Jonsdottir, R.A. Klein, Fluid Phase Equilib. 132 (1997) 117–137.
- [27] A.-H. Meniai, D.M.T. Newsham, Fluid Phase Equilib. 158–160 (1999) 327–335.
- [28] G. Perron, L. Couture, J.E. Desnoyers, J. Solution Chem. 216 (1992) 433–443.
- [29] A. Lancia, D. Musmarra, F. Pepe, J. Chem. Eng. Jpn. 29 (1996) 449–455.